Semiannual Status Report

for the period 88/11/1 through 89/4/30

on

Grant NAG 5-538

Studies of Regional and Global Tectonics and the Rotation of the Earth Using Very-Long Baseline Interferometry

Irwin I. Shapiro
Principal Investigator

Harvard College Observatory
60 Garden Street
Cambridge, Massachusetts 02138

(NASA-CR-185059) STUDIES OF REGIONAL AND GLOBAL TECTONICS AND THE ROTATION OF THE EARTH USING VERY-LONG BASELINE INTERFEROMETRY Semiannual Status Report, 1 Nov. 1988 - 30 Apr. 1989 (Harvard Coll.) N89-25534 Unclas G3/46 0212666

Reference: Grant NAG 5–538
Subject: Semiannual Status Report for 88/11/1 through 89/4/30

Progress

Data analysis

We have now almost completed the large reprocessing of the Mark III VLBI data set. Over 800 VLBI experiments have been analyzed in the last 6 months bringing our processed data set up to February, 1989 for IRIS, and November, 1988 for CDP experiments. We will request more data from both NGS and GSFC in early June.

Atmospheric delay calibration

We have submitted the results of Gunnar Elgered and our analysis of the WVR data from the Onsala Space Observatory. A preprint of the paper is attached.

Software conversion

Much of our effort recently and for the near future will focus on conversion of the VLBI analysis software from the HP 1000 to Unix based workstations. Given GSFC's experience recently of transferring the software between two different Unix machines, we hope that this transfer will go smoothly.

Papers

We have two papers about ready to be submitted to the Journal of Geophysical Research. These papers discuss our Kalman filter analysis of VLBI data and the theory of the Earth's nutation with particular emphasis on the effects of the solid inner core.

Geodesy by radio interferometry:

Water vapor radiometry for estimation of the wet delay

G. Elgered*, J. L. Davis+, T. A. Herring, and I. I. Shapiro

Harvard–Smithsonian Center for Astrophysics

60 Garden Street

Cambridge, MA 02138

* Now at: Onsala Space Observatory, Chalmers University of Technology, S–43900 Onsala, Sweden.

+ Now at: U S Geological Survey, 345 Middlefield Rd, MS 977, Menlo Park, CA 94025.

submitted to *J. Geophys. Res.*

Date: 22 May, 1989

ABSTRACT

An important source of error in very–long–baseline interferometry (VLBI) estimates of baseline length is unmodeled variations of the refractivity along the propagation path through the atmosphere. We present and discuss the method of using data from a water–vapor radiometer (WVR) to correct for the propagation delay caused by atmospheric water vapor. Data from different WVR's are compared with estimated propagation delays obtained by Kalman–filtering of the VLBI data themselves. The consequences of using either WVR data or Kalman filtering to correct for atmospheric delays at the Onsala VLBI site are investigated by studying the repeatability of estimated baseline lengths from Onsala to several other sites. The lengths of the baselines range from 919 to 7941 km. The repeatability obtained for baseline–length estimates shows that the methods of water–vapor radiometry and Kalman filtering offer comparable accuracies when applied to VLBI observations obtained in the climate of the Swedish west coast. It is also clear that VLBI observations made at low elevation angles should not be used if no estimations of the atmospheric delay are to be made for that site from the VLBI data. The "best" minimum elevation angle to allow depends on the accuracy of the *a priori* estimates of the total propagation delay, since the error in this delay increases with increasing air mass. For use of either WVR data or a model, based on the humidity and temperature at the ground, the best minimum is found to be either about 20° or about 35°, respectively.

1. INTRODUCTION

To correct for the "wet" atmospheric delay of radio signals, water–vapor radiometers (WVR's) have been developed for very–long–baseline interferometry (VLBI) experiments designed for estimation of geodetic parameters. This delay, although much smaller than the delay caused by the "dry" constituents of air, is—due to its variability in space and time—a major source of error in estimates of geodetic parameters such as baseline lengths.

WVR data can be treated as *a priori* information about the wet delay, *i.e.*, information obtained prior to least–squares estimation of site positions, *etc.* Other *a priori* data are ground measurements of humidity and temperature that can be used with a model to predict the wet delay. Due to poor mixing of wet and dry air, the accuracy of this type of model is expected to be too poor to be useful for our application. For comparison, however, we do use a model of this type [*Saastamoinen*, 1972]; we will refer to it as the ground–based model.

Ideally we would like to estimate the wet delay with an uncertainty much less than 30 ps ($\approx$10 mm equivalent path), which is the typical uncertainty of the group–delay data. It appears that there is no practical possibility for achieving this level of accuracy other than by use of a remote sensing instrument, such as the WVR. However, it is also possible to estimate a correction to *a priori* delays simultaneously with estimating geodetic and other parameters from the VLBI data. For example, we can estimate a mean zenith bias for an entire observing session or values of samples of, say, an assumed random (Markov) process [*Herring et al.*, 1989a] representing the wet delay.

This paper addresses the utility of WVR's in geodetic VLBI experiments. The experiments analyzed here all consist of dual–frequency band observations (S and X band). The experiment setup and the data flow are described by *Clark et al.* [1985]. Before giving our results, we provide a general background discussion of atmospheric delays and water–vapor radiometry. Thereafter, we describe the different WVR's that have been used to collect the data we analyzed. The results are presented in two ways. First, we compare the inferred wet–delay variations from the WVR to estimates obtained from a Kalman filter for several experiments. Second, we compare the repeatability of estimated baseline lengths obtained using different methods to correct for the atmospheric delays. Since the longest timespan of WVR data associated with geodetic VLBI experiments was obtained at the Onsala Space Observatory in Sweden, we present series of estimates of lengths of baselines from Onsala to other sites in the U. S. and Europe.

2. THE ATMOSPHERIC DELAY AND WATER–VAPOR RADIOMETRY

The delay through the neutral atmosphere depends on two terms [*Davis et al.*, 1985]. The first is called the "hydrostatic" (or "dry") delay. Its value ΔL_h in the zenith direction, expressed in meters, is

$$\Delta L_h = (0.0022768 \pm 0.0000015) \frac{P_\circ}{f(\Phi, H)} , \tag{1}$$

where $P_\circ$ is the total pressure at the ground in mbar and where

$$f(\Phi, H) = (1 - 0.00266 \cos 2\Phi - 0.00028H) \tag{2}$$

is used to model the variation of the acceleration due to gravity with latitude Φ and the height of the station H, in km, above the (international) ellipsoid, although the results are not sensitive to the specific ellipsoid chosen. The uncertainty given for the hydrostatic delay is the root sum square of the effects on it of the uncertainties in *(1)* the measurements of the refractivity of dry air [*Boudouris*, 1963] (which is about sixfold larger than the uncertainty given by *Thayer* [1974]), *(2)* the acceleration due to gravity, *(3)* the universal gas constant, and *(4)* the variability of the dry mean molar mass. Any departures from hydrostatic equlibrium are, however, not included.

The elevation–angle dependence of the hydrostatic delay is modeled using a "mapping function", the accuracy of which is improved if other meteorological measurements, such as of the ground temperature, are used (see, *e.g., Hopfield* [1971]). The mapping function we used for the hydrostatic delay in this study is presented by *Davis et al.* [1985].

The second term of the total delay is the wet delay, ΔL_w, which, defined consistently with the hydrostatic delay (1), can be written as

$$\Delta L_w = 10^{-6}\left[(17 \pm 10)\int_0^\infty \frac{e}{T}\,ds + (3.776 \pm 0.03) \times 10^5 \int_0^\infty \frac{e}{T^2}\,ds\right] , \quad (3)$$

expressed in the same units as is the path, s; T is the temperature in K; and e is the partial pressure of water vapor in mbar. The standard deviations are from the experimental determinations of these constants (*Boudouris* [1963]; see *Davis et al.* [1985] for discussion). This wet delay is determined mainly by the amount of water vapor along the atmospheric path, corresponding to the integration path in Equation (3).

The WVR measures the emission from the sky at two (or more) well separated frequency bands with one of the bands near the water–vapor emission line which is centered between 22 and 23 GHz. The WVR intensity output, for the band closest to the center of this line, will depend on the amount of water vapor in the direction the WVR antenna is pointed. A second frequency band is needed to correct for emission caused by liquid water, which occasionally can be larger than the vapor contribution (even at the center of the water–vapor line). Using the Rayleigh–Jeans approximation and the equation of radiative transfer [*Chandrasekar*, 1960], we can write the sky–brightness temperature measured by the WVR as

$$T_s = T_{bg} e^{-\tau_\infty} + \int_0^\infty T(s)\ \alpha(s)\, e^{-\tau(s)}\ ds \quad , \tag{4}$$

where T_{bg} is the "background" radiation (*i.e.*, from outside the earth's atmosphere). In the frequency band relevant to WVR's T_{bg} is due primarily to the cosmic background radiation. $T(s)$ is the physical temperature of the atmosphere along the path and $\alpha(s)$ is the (composite) attenuation coefficient due to water vapor, liquid water and oxygen. The parameter $\tau(s)$ is the corresponding opacity from the ground to the point s:

$$\tau(s) = \int_0^s \alpha(s')\ ds' \ . \tag{5}$$

When s is equal to infinity the opacity is written as τ_∞. The attenuation coefficient for each of the atmospheric constituents has a unique frequency dependence, which makes it possible to separate approximately the effects due to oxygen, water vapor, and liquid water.

When studying Equations (3)–(5) it becomes clear that by making some approximations we can formulate several (non–unique) algorithms which will allow us to estimate the wet delay from WVR measurements of sky–brightness temperature. It is possible to take many different approaches. Generally, the development of the algorithms assumes that the atmosphere is optically thin at the frequencies used by the WVR, and thus, T_s can be used to obtain an estimate of τ_∞. The opacity, or similar quantity such as linearized brightness temperature, is then related to path delay by an integral of the form,

$$\Delta L_w = \int_0^\infty W(s)\alpha(s)\ ds \quad , \tag{6}$$

where, $W(s)$, the "weighting function", is given by

$$W(s) = \frac{10^{-6}\left[17\frac{e}{T} + 3.776 \times 10^5 \frac{e}{T^2}\right]}{\alpha(s)} \quad , \tag{7}$$

and where the ratio $\int_0^\infty W(s)\alpha(s)\ ds / \int_0^\infty \alpha(s)\ ds$ is the "atmosphere averaged" weighting function, $\overline{W}$. It is $\overline{W}$ which is empirically parameterized in terms of meteorological conditions, and which must be optimized for a particular site. Most algorithms do not try to relate the brightness temperature at a single frequency to ΔL_w, but rather form a linear combination of the brightness temperatures at two frequencies so that the effects of liquid water can be largely removed (see, *e.g.*, *Wu* [1979]). The contribution of the attenuation of oxygen is also usually removed based on empirical models for its dependence on surface pressure and temperature (see, *e.g.*, *Gaut* [1968]). While such constructions change the detailed dependencies of the quantities in $W(s)$, the dependence of $\overline{W}$ on meteorological conditions remains. Different wet–delay algorithms have been derived by *Resch* [1983], *Gary et al.* [1985], *Robinson* [1988], and *Johansson et al.* [1989]. These algorithms are derived for many VLBI sites used (or to be used) in geodetic experiments and most of them make use of meteorological parameters measured at the ground.

Let us define the "algorithm error" as the error of the wet delay inferred from noise free radiometer observables. The algorithm error can then be divided into two parts. The first part is a scatter which varies on time scales of hours to days. We obtain this error if we assume that the expressions for radio signal attenuation used to derive the algorithm are correct. Depending on the completeness of the parameterization of $\overline{W}$, this error source can vary between different algorithms. For the algorithms referred to above, the root–mean–square (RMS) error of this part, for the zenith direction, varies between 1 and 4 mm, depending on algorithm and site, for weather situations excluding rain or heavy rain–clouds. This error will change slowly with time since it depends on changes in the height profiles of temperature and humidity in the atmosphere. The typical rate of change, for the zenith direction, is 1–2 mm/12h but a few times per year it can approach 10 mm/12h (see *Elgered* [1989] and references above).

The second part of the algorithm error is due to errors in the attenuation coefficients. This part of the error should be common to all algorithms which use the same expressions for the attenuation coefficients. The uncertainty in the attenuation of oxygen is the least important and corresponds to an error in the inferred wet delay in the zenith direction of less than 2 mm [*Elgered*, 1989]. This value was derived by comparing the results from algorithms of the form described above using different attenuation coefficients for oxygen [*Meeks and Lilley*, 1963; *Snider and Westwater*, 1969; *Liebe*, 1985; *Liebe*, 1987; *Rosenkranz*, 1988].

The attenuation due to liquid water is assumed to be caused by Rayleigh scattering, in which case it is proportional to the square of the frequency. This frequency dependence is valid as long as the sizes of the liquid water drops are much smaller than the wavelength of the attenuated signal [*Staelin*, 1966]. For all the WVR's used for geodetic VLBI, the "cloud correction band" is centered at about 31 GHz (wavelength $\approx$ 10 mm). If the size of the drops in the atmosphere are not, say, a few tenths of a millimeter or less, *i.e.*, negligible compared to the wavelength, dual–frequency type algorithms will overestimate the wet delay [*Westwater*, 1972]. An example of the effect of large drops is given in Figure 1, where the effect is further increased by the accumulation of water drops on the teflon–covers of the horn antennas. Our experience indicates that during rain, WVR data are of no use for the calculation of accurate wet–delay corrections.

When it is not raining the uncertainty in the attenuation due to water vapor appears to be the limiting factor. There are a number of published formulas for this attenuation [*Staelin*, 1966; *Waters*, 1976; *Liebe*, 1985; *Liebe*, 1987], and a lower bound on the errors in the estimates of ΔL_w obtained by radiometric techniques can be obtained by comparing algorithms derived with different expressions for the water–vapor attenuation. Such studies indicate that errors in ΔL_w of 4–8%, with the uncertainty increasing with decreasing temperature, are likely [*Elgered*, 1989]. Even a 4% error is, however, not negligible. Zenith wet delays of between 100 mm and 300 mm are not unusual in the temperate summer. (Here, and hereafter, we express delays in terms of equivalent path length.) For typical elevation angles of about 30°, we will then obtain errors of the order of 10–30 mm in our estimated delay corrections. These errors are large when compared to the uncertainties of individual VLBI group delay measurements which are of order 10 mm or less.

3. BRIEF DESCRIPTION OF WATER-VAPOR RADIOMETERS FOR GEODETIC VLBI

Responsibility for the design and manufacture of WVR's specifically for use in geodetic VLBI experiments was assigned by the National Aeronautics and Space Administration (NASA) in the mid 1970's to the Jet Propulsion Laboratory (JPL) in Pasadena, CA, where seven WVR's were subsequently built [*Resch et al.*, 1985]. Independently, at the Onsala Space Observatory in Sweden, one WVR was built [*Elgered and Lundh*, 1983]. Later four of the JPL instruments (known as R–series WVR's) were upgraded, and a new more compact (J–series) WVR was made at JPL [*Janssen*, 1985]. More J–series WVR's are now being built and another, independently designed, WVR is being built at the Geodetic Institute in Bonn for use at the VLBI station in Wettzell, FRG [*Reichert*, 1985].

The different WVR's that have been used in Mark–III VLBI experiments are briefly described in Table 1. System noise–temperatures are all about 600 K. The WVR's are all fully steerable in azimuth and elevation, but the slew speeds are quite different. Even though all antennas used for VLBI observations typically slew at 0.5–2°/s, it is an advantage to have a higher slewing speed for the WVR. Instrumental calibrations are generally formulated as corrections to the temperatures of reference loads or noise–diodes and are obtained by frequently performing elevation scans (also known as "tip–curves"). This procedure should be more successful if the WVR slews sufficiently fast to allow time between the VLBI observations for making tip–curves.

The tip–curve method is sensitive to any inhomogeneities in the atmosphere; but, provided that tip–curves are carried out at different azimuth angles, even simple gradients are easily detected and modeled. If the atmosphere is very inhomogeneous, which is often the case when significant amounts of liquid water are present, the noise in the tip–curve data becomes very apparent and the data can be downweighted before using them in the calibration procedure.

4. INFERRING WET DELAYS FROM WVR DATA AND FROM A KALMAN FILTER

When a Kalman filter is used to estimate the atmospheric delay [*Herring et al.*, 1989a], the normal procedure is to use the measured ground pressure to calculate the hydrostatic delay using Equations (1) and (2), and to estimate an additional delay which is then assumed to be equal to the wet delay. The wet delay estimated using the Kalman filter will, therefore, have an additional uncertainty arising from errors in the inferred hydrostatic delay. Since the water vapor has a different distribution with height than has the dry air, a special "wet mapping function" has to be used to calculate the partial derivatives in the estimation process. A mapping function for the elevation–dependence of the wet delay presented by *Chao* [1972] was used in the analysis.

We have compared the two methods—Kalman filter and WVR—at different sites involving different WVR's. Figures 2–4 show the equivalent zenith wet delay inferred from WVR data and estimated, using the Kalman–filter technique, from the VLBI data themselves. The error bars for the WVR data have been omitted. They vary, mainly as a function of the elevation angle of the observation, between 5 and 8 mm for the old R–series WVR and between 2 and 4 mm for the other instruments. In addition to these random errors, there are the biases in the measurements and in the inversion algorithm both of which contribute to the overall uncertainty of the WVR–inferred wet–path delays. The error bars for the VLBI estimates do not account for errors in either the zenith value or the mapping function of the hydrostatic delay.

In Figure 2 the WVR data are from the old R–series used at the Haystack Observatory, MA; Figure 3 shows the same type of comparison for an upgraded R–series WVR at the Mojave site, located in the Mojave desert in California. Figure 4 shows the result from three contiguous observing sessions: one "Atlantic" experiment within NASA's Crustal Dynamics Project (CDP) [*Coates et al.*, 1985], including antennas at Westford (MA), Onsala (Sweden), and Wettzell (Federal Republic of Germany); one "IRIS" (International Radio Interferometric Surveying [*Carter et al.*, 1985]) experiment, including antennas at Westford, Fort Davis (TX), Richmond (FL), Onsala, and Wettzell; and one "Polar" (CDP) experiment, including antennas at Kashima (Japan), Fairbanks (AK), Mojave, Westford, Onsala, and Wettzell.

5. ON THE ACCURACY OF THE ESTIMATED PROPAGATION DELAY

In each of the comparisons shown in Figures 2–4 both sets of estimates often exhibit similar short–term variations for the wet delay, but with an apparent long–term bias. We have studied these biases for the Onsala site using a set of 119 Mark–III VLBI experiments in which WVR and VLBI data are both available at the Onsala site for more than approximately half of each experiment. These experiments were carried out between July 1980 and June 1988. The WVR data were used with the algorithm presented by *Johansson et al.* [1989] for estimating the wet delay. We used ground–pressure measurements together with the WVR data to determine the propagation delays at Onsala, but during the solution estimated one constant correction to the equivalent delay in the zenith direction for each experiment. At all other sites the atmospheric delays were estimated by assuming that these delays could be represented by a random–walk stochastic process. The clocks at all sites were estimated using a combined random–walk and integrated–random–walk stochastic process [*Herring et al.*, 1989a]. The statistical parameters of the Markov process used for the atmospheric delay estimation were obtained from previous analyses of the rate residuals for each experiment [*Herring et al.*, 1989a]. Ideally the estimate of this additional delay in the zenith direction would be zero for each experiment. However, there are several sources of error which will influence the result. (The estimated errors are given as "root–mean–square (RMS)" and "bias" for a 24 hour period in each relevant case. The signs of the biases are unknown; their magnitudes are inferred approximately from the spread in published values or from experimental evidence.)

1. Error in the inversion algorithm used with the WVR data, due to approximations of the atmospheric profiles of pressure, temperature, and humidity (2 mm RMS in the zenith direction for the algorithm used with this data set [*Johansson et al.*, 1989]).

2. Error in the inversion algorithm used with the WVR data, due to uncertainties in the attenuation coefficients of water vapor (a bias of approximately 4–6% of the wet delay [*Elgered*, 1989]).

3. WVR instrumental error (RMS 3–5 mm, bias up to 5 mm).

4. Uncertainty of the wet refractivity (the constants in Equation (3), bias of 1% of the wet delay [*Boudouris*, 1963]).

5. Error in the total pressure measurement at Onsala (estimated error: 1 mbar, corresponding to 2 mm in equivalent zenith delay). This error is a bias during an experiment but could vary over time scales of months as determined by comparison of Onsala's barometer with nearby (<40 km distant) airport barometers.

6. Uncertainty in Equation (1) for the hydrostatic delay (bias of 0.1%, corresponding to 2 mm in equivalent zenith delay).

7. Violation of hydrostatic equilbrium in the atmosphere. Such errors should be important (larger than 1 mm in equivalent zenith delay) only when very strong winds exist [*Holton*, 1979]. In this data set, before March 1987, there are no data taken at Onsala when the wind exceeded 13 m/s at the ground due to a wind–speed limit for antenna operation. However, this surface–wind–speed condition does not exclude the possibility of high altitude winds affecting our results.

8. Any unmodeled effect in the VLBI data which could affect the estimate of the excess propagation delay.

9. Errors in the mapping functions. The hydrostatic mapping function which is used to map the hydrostatic (or dry) delay from the zenith direction to the elevation angle of the observation. (RMS at 10 degrees elevation angle is about 10 mm, which projects through our estimator to yield approximately 5 mm RMS errors in the estimated zenith wet delay.) The error in the wet mapping function is believed to be of the same magnitude. The biases presented in Figure 4 were reduced approximately 5 mm by using hydrostatic and wet mapping functions

derived from radiosonde profiles obtained at Gōteborg–Landvetter Airport 38 km from Onsala.

Three sets of solutions are presented in Figure 5. Each solution uses a different minimum (cut–off) elevation angle for the observations made at Onsala. The effect of an error in the mapping function is expected to be larger at low elevations, which should be reflected in the estimated mean bias. Of course, the uncertainty of the estimated zenith bias increases rapidly with increasing cut–off angle. We obtain a rather large uncertainty (2.3 mm) of the estimated bias for a 25° cut–off in elevation angle. This fact, together with there being no significant difference in the mean biases obtained in the first two solutions (no cut–off and 15° cut–off), imply that it is not possible to explain the bias solely in terms of errors in the mapping functions.

The errors associated with the estimates of wet delay are primarily fractional errors and can not alone explain the results in Figure 5: a distinguishable bias of about 10 mm virtually constant with time. Fractional errors will cause the estimates of the wet delay to have errors which increase in the summer, when the wet delay is large, and decrease in the winter. However, an instrumental bias of the WVR could be at least partly responsible. To address the issue of instrumental biases, side–by–side comparisons of ASTRID (Table 1) and a new J–series radiometer (J03) were made at Onsala in June and July 1988, in an experiment organized by the Onsala Space Observatory and NASA/GSFC. A preliminary analysis of these data by one of us (GE) and personnel from NASA/GSFC, has shown that the biases between these instruments varied between 0 and 8 mm, on time scales of days, for the duration of the comparison [*Clark, private communication*, 1989]. The preliminary estimates of the mean bias and RMS difference between the results from the two radiometers are 1 and 5 mm, respectively. When it is completed, a detailed analysis of these data will be presented elsewhere.

Another source of error that deserves comment is the uncertainty in the observed total ground pressure. The observed pressures at the Onsala site used in this data set have been compared to the results from other pressure sensors in the area and corrected, when necessary. Thereafter, the pressure was referred to the height at which the signals are referenced within the radio telescope. We believe this procedure has resulted in an uncertainty of the pressure measurements of about 1 mbar corresponding to an equivalent zenith delay standard error of about 2 mm.

Finally, we note that by combining the errors discussed above we could reproduce the observed 10 mm bias in the estimated zenith delay, but this reproduction would require the sum of many small terms. Hence, the overall bias can be reduced significantly only by reducing the size of many of the individual sources of error described above.

6. USING WVR DATA AND LOW ELEVATION ANGLE OBSERVATIONS

Low elevation angle observations are not important when atmospheric delay corrections are not estimated [*Herring*, 1986]. Such observations will actually degrade the accuracy of the (other) estimated parameters if either there is a bias error in the atmospheric delay calibrations or if mapping–function errors are present [*Davis et al.*, 1985].

Independent of the sources of the bias discussed in the previous section, it is important to study the resulting repeatability of estimated baseline lengths for different elevation cut–off angles when no atmospheric delays are estimated for the sites that have WVR's. Some results are shown in Figure 6 where again the set of 119 experiments involving WVR data at Onsala is used. For each set of solutions made, for a given elevation cut–off angle, the weighted root–mean–square (WRMS) scatter of baseline lengths about the estimated slope is presented. The WRMS value is used as a measure of repeatability. In these solutions no atmospheric parameters are estimated, and there is a small improvement in repeatability for all baselines (excluding Onsala–Haystack) when we discard low elevation data. The effect is larger for the longer baselines since the error made in the local vertical coordinate affects the baseline length more in these cases. Although the optimum cut–off angle is not identical for the different baselines, a value of 20° seems reasonable for all cases. Because of ground noise pick–up, it should be noted that an elevation angle of 20° is approximately equal to the lowest elevation that can be usefully used by all of the WVR's described in this paper.

To show the cut–off effect more clearly, we have used the ground–based model instead of the WVR data; the results are presented in Figure 7. The expected errors accompanying the use of this model, averaged over a year, is about 20 mm RMS in equivalent zenith delay for the Swedish west coast climate [*Elgered and Lundqvist*, 1984]. The main part of this error will show up as a bias during a 24 hour observing session. In this case an elevation cut–off angle of about 35° is recommended. Note that the data deleted in this study are only those for observations made below the elevation angle cut–off at Onsala. If the cut–off criterion had been applied at other sites as well we would have had a much larger data loss (especially for the long baselines), implying a more rapid increase of the WRMS for higher cut–off angles.

7. REPEATABILITY OF ESTIMATED BASELINE LENGTHS: COMPARISONS BETWEEN USING WVR DATA AND KALMAN FILTERING

The set of 119 experiments was analyzed several more times, each time with a different method used to correct for the wet delay at Onsala, but with the atmospheric delays for all other sites (as well as the clocks for all sites) modeled as Markov processes.

The estimated mean rates of change of the baselines from these analyses are presented in Table 2 as are all the WRMS scatters about these slopes. Based on the results presented in Figures 6 and 7, an elevation cut–off angle was applied when either WVR data or the ground–based model was used and no estimates were made for the atmospheric delay at Onsala. The repeatability obtained is about the same in all cases which involve either the use of WVR data as *a priori* information or the estimation of the atmospheric delays based on their being Markov processes. The differences of the estimated rates are small compared to their estimated uncertainties. Since the estimates of the rates are correlated for the different solutions because they share common data, we expect, based on the arguments given in *Davis et al.* [1985, appendix B], that the uncertainties of the differences should be equal to or greater than the square root of the difference of the estimated variances for each rate estimate. *Davis et al.* showed that, when parameters are estimated from two sets of data with one of the sets being a subset of the other, the variance of the difference of the parameter estimates is the difference of the variances from the two estimations. (The sense of the difference is the variance from the smaller data set minus the variance from the larger.) An extension of the arguments given there can be used to show that the same rule applies when different numbers of parameters are estimated, provided the smaller set of parameters is a subset of the larger set. In our case, the solution with the larger number of parameters also has the largest number of observations, and thus we can establish only the lower bound on the variance of the difference as the difference of the variances. There are complications introduced by our scaling of the variances so that χ^2 per degree-of-freedom is unity; however, in most cases these scaling factors were of similar size. Thus, the lower bound is approximately correct.

For two baselines (Onsala–Haystack and Onsala–Owens Valley), it appears better to estimate a constant correction to the zenith delay inferred from the WVR data than to discard low elevation observations. In the case of Onsala–Haystack, we know from Figure 6 that inclusion of the low elevation data actually yielded a lower WRMS, even with no atmospheric bias estimated. Note that the 90% confidence intervals are relatively large for these two baselines and that they were based on more data from earlier epochs than were the other baselines (see the mean epochs given in Table 2). The quality of WVR data, as well as of VLBI data, have improved since 1980.

The change of accuracy of the data with time is further illustrated in Figure 8 where we have combined all the results from Onsala to Haystack and to Westford. Note that either Haystack or Westford or both have been involved in all the 119 experiments analyzed in this paper. The WRMS about the "best–fit" slope for the last 37 experiments (August 1986–June 1988) is 9.8 mm, when the WVR data are used, and 12.0 mm when, instead, the wet delays are estimated.

To better understand the differences between the solutions with and without the WVR data used, we have compared the estimates of the coordinates of Onsala for the two types of solution shown in Figure 8. We will refer to these as the Markov and WVR solutions. In general, studies of station coordinates are complicated by our uncertain knowledge of Earth rotation parameters. To avoid the complications of *(a)* the errors introduced by interpolating Earth rotation data, and *(b)* the effects of correlations between the Earth rotation parameters (which are largely determined by VLBI data) and our data, we choose to restrict our data set to those experiments which included Wettzell and at least two other sites. The positions of Onsala were then determined in a coordinate system defined by the other sites in the network. These other sites were moved in a such a way that the coordinate system they defined should be fixed relative to North America (see *Herring et al.* [1989b]). The fifty–four estimates of Onsala's position in its local North, East and Up coordinate system are shown in Figure 9 for the Markov and WVR solutions. The WRMS scatters of the results from these two solutions are very similar for each component. In particular, for the Markov solution, the WRMS scatter of the North component, which is the component least affected by errors in our estimates of the Earth rotation parameters, is 3.3 mm; of the East component 6.9 mm; and of the height 20.1 mm. The corresponding values for the WVR solution are 3.2, 7.0, and 22.2 mm. Here we see no improvement in the repeatability of the estimates of the heights when the WVR data are used, although this lack of improvement is probably due largely to a single experiment in September 1987, for which the WVR data had large gaps due to rain. If this experiment is removed, then the WRMS scatter of height estimates from the WVR solution reduces to 20.4 mm. In examining Figures 8 and 9, we note that the Markov solutions have several experiments with large residuals relative to their error bars; their counterparts for the WVR solution are not anomalous. We have examined some of these experiments in detail, especially those in June and October of 1987. The estimates of the heights from all of these experiments show a large dependence on the minimum elevation angle of the Onsala data included in the solution—as low elevation angle data are removed the estimates from solutions with and without atmospheric parameters estimated approach values consistent with the trend of the best–fit straight line, but from opposite sides. The WVR solutions shown in the figure are not greatly affected by this characteristic because the data below 20° elevation angle were not used. We interpret this behavior as being due to an error in the mapping function for the hydrostatic delays. We are now undertaking a detailed study of some of these experiments so that we can gain a better understanding of the meteorological conditions which lead to such errors in the mapping functions.

There is a mean difference of -17±2 mm in the heights estimated from the Markov and WVR solutions. This mean difference is consistent with the mean difference in the estimates of the baseline length between Westford/Haystack and Onsala, and, presumably, arises from the same source which causes the -10.7 mm average zenith delay bias when the atmospheric delay is fully calibrated. The relationship between the zenith delay bias and the height difference is consistent with the source of the bias either being an actual bias in the calibration or an artifact of a (constant) error in the mapping function for the hydrostatic delay.

8. INTERPRETATION OF RESULTS

The primary aim of this paper is to discuss estimates of the wet delay obtained from water vapor radiometry. However, there are apparently geophysical signals in the results we have presented which we now examine. The following discussion is our tentative interpretation of these results; there are still many issues we need to address before we will be satisfied that we fully understand these signals. Before we start our discussion, we will clarify the meaning of the error bars accompanying the results presented thus far. We believe these error bars represent the random–noise contribution to our estimates of the geodetic parameters; thus, deviations between results which would be judged significant based on these errors bars, we believe are significant—but not necessarily of **geophysical** significance. Significant deviations could well represent unmodeled systematic errors in our data analyis, and much of our discussion will be concerned with trying to separate geophysical signals from systematic errors.

The estimates of the mean rate of change of the lengths of baselines connecting North America to Onsala are smaller than the rates expected from the million–year averaged geologic plate–motion models. In particular, the average rate of change from the geologic models for the Westford–to–Onsala baseline is 17.2±1mm/yr—about 4 mm/yr greater than the rate we find. The study of the corresponding three–dimensional coordinates indicates that this lower rate, at least for the last 4 years, is due to the estimated height of Onsala decreasing at an average rate of about 13±2–3 mm/yr. This result is contrary to current geophysical theories of post–glacial rebound which would predict an **increasing** height of Onsala at a rate of 3 to 10 mm/yr [*Peltier*, 1986; *Wagner and McAdoo*, 1986]. We are studying the possibility that other effects are causing an apparent vertical fall of this site. Perhaps relevant here is the origin of the ≈10 mm zenith–delay residual which is found after we have purportedly "fully" calibrated the total atmospheric delay with the WVR data. But, given that this bias has been constant, with no apparent seasonal signatures, for over 8 years, it seems unlikely that its cause would introduce a secular rate of change of height. Errors in modeling the mapping function for the hydrostatic delay could introduce time dependent biases in the estimates of height; however, the Markov and WVR solutions each showing about the same rate of change, despite these solutions having oppositely–signed sensitivities to this type of error, seems to rule out this possibility. Thus, we have as yet no plausible source of systematic error that would account for the discrepancy.

The estimates of height from the WVR solution also show some unexpected systematic behavior, especially in 1984 when all of the estimates are below the trend of the best–fit straight line. Given the sensitivity of this type of solution to errors in the calibrated zenith delay, even with data below 20° excluded from the solution, we are extremely reluctant to attribute this behavior to actual changes in the motion of the site, especially since we do not see such pronounced behavior in the Markov solution, which is insensitive to errors in the *a priori* calibration of the zenith delays. There are, however, other indications of temporal variations in the height of Onsala or in the source(s) of systematic error. The average rate of change of the Haystack/Westford–Onsala baseline prior to late 1984 was 17.4±1.7 mm/yr for the Markov solution, a value consistent with that given in *Herring et al.* [1986]. The estimates after this date have an average rate of change of only 8.8±1.5 mm/yr. The corresponding rate estimates for the WVR solution are 18.3±1.9 and 9.8±1.3 mm/yr. However, despite these large, and consistent signals, we are certainly not convinced that these differences result from a change in the motion of Onsala, given the as yet incompletely understood systematic errors affecting our results. In particular, from this data set we can not discount the possibility that the Westford site is responsible for the changing rate. A complete analysis of the VLBI data set, discussed in *Herring et al.* [1989b], does seem to rule out this possibility.

9. CONCLUSIONS

WVR data and the Kalman–filter approach for the "wet" delay calibration give comparable repeatability of estimated baseline lengths when used for the Onsala VLBI site. We find from our data set that the "best" elevation cut–off angle when WVR data are used is about 20°. Low elevation angles are, nevertheless, important since they imply a better geometry and are necessary to obtain accurate results if atmospheric delays are to be estimated [*Davis et al.*, 1989]. Such estimates may be necessary if, for example, a WVR is not available at a site or if it rains during a portion of an experiment, thus making the WVR data useless for our application. It is, therefore, of the greatest importance to minimize possible biases in the total atmospheric delay inferred from ground pressure measurements and WVR data so that data from observations at low elevation angles can be used without degradation of the accuracy.

Most of the results in this paper involve WVR data taken with one specific instrument operating in the specific climate of the Swedish west coast. This WVR is not a state–of–the–art instrument. Moreover, the daily variations in the wet delay at Onsala are expected to be smaller than those present at many other geodetic VLBI sites. Since the uncertainties of the estimated parameters increase if a more variable wet delay is to be estimated by a Kalman filter (see *Herring et al.* [1989a]), use of an accurate WVR instrument at a more humid site should yield larger improvements in the repeatability of the estimates of geodetic parameters than those obtained in this study.

Given the repeatability obtained using the Kalman–filter technique and the cost of a WVR, it may prove useful to have a WVR only at sites frequently used and/or where the expected wet delay variations are large. The WVR data can then also be used to check simultaneous Kalman–filter estimates of the wet delay, and to guard against other unmodeled errors in the VLBI data being absorbed into atmospheric delay–estimates. However, since the Kalman filter technique is sensitive to mapping–function errors, it may be necessary to use either a WVR or frequent radiosonde launches at each site to obtain the most accurate geodetic VLBI results.

ACKNOWLEDGMENTS

This work was supported by the Air Force Geophysics Laboratory, contract F–19628–86–K–0025; NASA grant NAG5–538; NSF grant EAR–86–18989; and the Smithsonian Institution.

REFERENCES

Boudouris, G., On the index of refraction of air, the absorption and dispersion of centimeter waves by gases, *J. Res. Natl. Bur. Stand.*, *67D*, 631–684, 1963.

Carter, W.E., D.S. Robertson, J.R. MacKay, Geodetic radio interferometric surveying: applications and results, *J. Geophys. Res.*, *90*, 4577–4587, 1985.

Chandrasekhar, S., *Radiative transfer*, Dover, New York, 393 pp., 1960.

Chao, C.C., A model for tropospheric calibration from daily surface and radiosonde balloon measurements, *Tech. Mem. 391-350*, Jet Propul. Lab., Pasadena, California, 1972.

Clark, T.A., B.E. Corey, J.L. Davis, G. Elgered, T.A. Herring, H.F. Hinteregger, C.A. Knight, J.I. Levine, G. Lundqvist, C. Ma, E.F. Nesman, R.B. Phillips, A.E.E. Rogers, B.O. Rõnnãng, J.W. Ryan, B.R. Schupler, D.B. Shaffer, I.I. Shapiro, N.R. Vandenberg, J.C. Webber, and A.R. Whitney, Precision geodesy using the Mark-III very-long-baseline interferometer system, *IEEE Trans. Geosci. Remote Sensing*, *GE-23*, 438–449, 1985.

Coates, R.J., H. Frey, J. Bosworth, and G. Mead, Space-age geodesy: the NASA crustal dynamics project, *IEEE Trans. Geosci. Remote Sensing*, *GE-23*, 360–368, 1985.

Davis, J.L., T.A. Herring, I.I. Shapiro, A.E.E. Rogers, and G. Elgered, Geodesy by radio interferometry: effects of atmospheric modeling errors on estimates of baseline length, *Radio Science*, *20*, 1593–1607, 1985.

Davis, J.L., T.A. Herring, and I.I. Shapiro, Geodesy by radio interferometry: estimates of relative position obtained from transcontinental "low elevation-angle" VLBI experiments, *J. of Geophys. Res.*, 1989, this volume.

Elgered, G., and P. Lundh, A dual channel water vapor radiometer system, *Res. Rept. No. 145*, Chalmers University of Technology, Research Laboratory of Electronics and Onsala Space Observatory, 17 pp., 1983.

Elgered, G., and G. Lundqvist, A three-year study of radio wave propagation delays due to tropospheric water vapor, *IEEE Trans. Antennas Propagat.*, *AP-32*, 390–395, 1984.

Elgered, G., Tropospheric radio path delay from ground-based microwave radiometry, in *Atmospheric Remote Sensing by Microwave Radiometry*, edited by M. Janssen, Wiley & Sons, in press, 1989.

Gary, B.L., S.J. Keihm, and M.A. Janssen, Optimum strategies and performance for the remote sensing of path delay using ground-based microwave radiometers, *IEEE Trans. on Geoscience and Remote Sensing*, *GE-23*, 479–484, 1985.

Gaut, N.E., Studies of atmospheric water vapor by means of passive remote sensing, Tech. Rept. 467, MIT Research Lab. of Electronics, Ph.D. Thesis, 1985.

Herring, T.A., I.I. Shapiro, T.A. Clark, C. Ma, J.W. Ryan, B.R. Schupler, C.A. Knight, D.B. Schaffer, N.R. Vandenberg, H.F. Hinteregger, A.E.E. Rogers, J.C. Webber, A.R. Whitney, G. Elgered, G. Lundqvist, B.O. Rõnnãng, B.E. Corey, and J.L. Davis, Geodesy by radio interferometry: evidence for contemporary plate motion, *J. Geophys. Res.*, *91*, 8341–8347, 1986.

Herring, T.A., Precision of vertical position estimates from VLBI, *J. Geophys. Res.*, *91*, 9177–9182, 1986.

Herring, T.A., J.L. Davis, and I.I. Shapiro, Geodesy by radio interferometry: The application of Kalman filtering to the analysis of VLBI data, *J. of Geophys. Res.*, 1989a, this volume.

Herring, T.A., J.L. Davis, and I.I. Shapiro, Geodesy by radio interferometry: Analysis of the Mark III VLBI data set: 1980–1989, to be submitted to *J. Geophys. Res.*, 1989b.

Holton, J.R., *An introduction to dynamic meteorology*, 2nd ed., Academic Press, Orlando, 391 pp., 1979.

Hopfield, H.S., Tropospheric effect on electromagnetically measured range: prediction from surface weather data, *Radio Science*, *6*, 357–367, 1971.

Janssen, M.A., A new instrument for the determination of radio path delay variations due to atmospheric water vapor, *IEEE Trans. Geosci. Remote Sensing*, *GE-23*, 485–490, 1985.

Johansson, J.M., G. Elgered, and J.L. Davis, Geodesy by radio interferometry: Optimization of wet path delay algorithms using microwave radiometer data, *in preparation*, 1989.

Liebe, H.J., An update model for millimeter wave propagation in moist air, *Radio Science*, *20*, 1069–1089, 1985.

Liebe, H.J., A contribution to modeling atmospheric millimeter-wave properties, *Frequenz*, *41*, 31–36, 1987.

Meeks, M.L., and A.E. Lilley, The microwave spectrum of oxygen in the Earth's atmosphere, *J. Geophys. Res.*, 68, 1683–1703, 1963.

Peltier, W.R., Deglaciation-induced vertical motion of the North American continent and transient lower mantle rheology, *J. Geophys. Res.*, *91*, 9009–9123, 1986.

Reichert, G., Status of the SBF 78 water vapor radiometer, in *Proceedings of the 4 working group meeting on European VLBI for geodesy and astrometry*, edited by B.O. Rõnnãng and G. Tang, pp. 32–36, Onsala Space Observatory, 1985.

Resch, G.M., Inversion algorithms for water vapor radiometers operating at 20.7 and 31.4 GHz, *TDA Progress Report 42-76*, Jet Propulsion Laboratory, Pasadena, California, 12–26, 1983.

Resch, G.M., M.C. Chavez, N.I. Yamane, K.M. Barbier, and R.C. Chandlee, Water vapor radiometry research and development phase final report, *JPL Publication 85-14*, Jet Propulsion Laboratory, Pasadena, California, 1985.

Robinson, S.E., The profile algorithm for microwave delay estimation from water vapor radiometer data, *Radio Science*, *23*, 401–408, 1988.

Rosenkranz, P.W., Interface coefficients for overlapping oxygen lines in air, *J. Quant. Spectrosc. Radiat. Transfer*, *39*, 287–297, 1988.

Saastamoinen, J., Atmospheric correction for the troposphere and stratosphere in radio ranging of satellites, in *The Use of Artificial Satellites for Geodesy, Geophys. Monogr. Ser., 15*, edited by S.W. Henriksen *et al.*, pp. 247–251, American Geophysical Union, Washington, D.C., 1972.

Smith, D.E., R. Kolenkiewicz, P.J. Dunn, S.M. Klosko, E.EC. Pavlis, J.W. Robins, M.H. Torrens, R.G. Williamson, and S.K. Fricke, Vertical positioning in the laser tracking network, *EOS*, *69*, 1152, 1988.

Snider, J.B., and E.R. Westwater, Atmospheric attenuation at 15, 31, and 53 GHz, *ESSA Tech. Report ERL 156-WPL 11*, U.S. Department of Commerce, Boulder, Colorado, 1969.

Staelin, D.H., Measurements and interpretation of the microwave spectrum of terrestrial atmosphere near 1-centimeter wavelength, *J. of Geophys. Res.*, *71*, 2875–2881, 1966.

Thayer, G.D., An improved equation for the radio refractive index of air, *Radio Science*, *9*, 803–807, 1974.

Wagner, C.A., and D.C. McAdoo, Time variations in the Earth's gravity field detectable with geopotential research mission intersatellite tracking, *J. Geophys. Res.*, *91*, 8373–8386, 1986.

Waters, J.W., Absorption and emission by atmospheric gases, in *Methods of Experimental Physics*, vol. *12B*, edited by M.L. Meeks, pp. 142–176, Academic Press, New York, 1976.

Westwater, E.R., Microwave emission from clouds, *NOAA Technical Report ERL 219 - WPL 18*, U.S. Department of Commerce, National Oceanic and Atmospheric Administration, Environmental Research Laboratories, Boulder, CO., 1972.

Wu, S.C., Optimum frequencies of passive microwave radiometer for tropospheric path–length correction, *IEEE Trans. Antennas Propagat.*, *Ap–27*, 233-239, 1979.

Table 1. Water-wapor radiometers used in the Mark-III VLBI experiments.

	R-series[1]		New R-series[1]		J-series[1]			ASTRID[2]	
Frequencies [GHz]	20.7	31.4	20.7	31.4	20.7	22.2	31.4	21.0	31.4
Antenna beam-width [°]	7	7	7	7	9	9	7	6	6
Reference load temperatures [K]	313/413		313/413		313 + noise-diode			77/313 or 313/360[3]	
IF Bandwidth (DSB) [MHz]	5–100		10–110		40–200			5–500	
Slewing speed AZ,EL [°/s]	1.5, 1.5		7.5, 6.6		12, 60			1.7, 1.7	

[1] See text.
[2] The WVR at the Onsala site (Atmospheric Sky Temperature Radiometer for Interferometric Delay corrections).
[3] Referred to as "cold" or "hot" mode. The WVR was running in hot mode during six of the 119 experiments analyzed in this study.

Table 2. Baseline length repeatability

Baseline: Onsala to	Method used to correct for the wet delay at Onsala[1] *A priori*	Adjustment	Slope[2] (mm/year)	WRMS[3] about slope (mm)
Wettzell	None	Bias	-2.1±0.5	5.1
(72 experiments,	None	Markov	-1.9±0.4	4.1
919 km, mean	Model(35°)	None	-2.4±0.7	6.3
epoch 1987.0)	Model	Bias	-2.4±0.5	4.8
	Model	Markov	-1.8±0.4	4.3
	WVR (20°)	None	-1.6±0.4	4.0
	WVR	Bias	-1.4±0.5	4.4
	WVR	Markov	-1.6±0.4	4.2
Haystack	None	Bias	14.5±1.3	14.1
(30 experiments,	None	Markov	15.2±1.2	12.1
5600 km, mean	Model(35°)	None	14.7±2.3	24.8
epoch 1984.0)	Model	Bias	12.0±1.8	18.5
	Model	Markov	15.4±1.2	11.3
	WVR (20°)	None	16.3±1.3	13.3
	WVR	Bias	14.6±1.2	11.5
	WVR	Markov	15.4±1.3	12.0
Westford	None	Bias	11.6±1.6	20.9
(96 experiments,	None	Markov	12.9±1.0	13.9
5601 km, mean	Model(35°)	None	12.0±1.5	20.8
epoch 1986.8)	Model	Bias	11.2±1.4	19.0
	Model	Markov	12.8±1.0	13.7
	WVR (20°)	None	13.3±0.9	12.3
	WVR	Bias	13.3±1.1	14.6
	WVR	Markov	13.5±1.0	14.0
Richmond	None	Bias	4.4±3.3	21.2
(32 experiments,	None	Markov	4.4±3.3	21.2
7307 km, mean	Model(35°)	None	6.4±5.7	38.4
epoch 1986.9)	Model	Bias	4.4±3.6	23.0
	Model	Markov	4.8±3.4	22.1
	WVR (20°)	None	5.6±3.1	20.6
	WVR	Bias	7.9±3.5	22.3
	WVR	Markov	6.8±3.3	21.5
OVRO	None	Bias	12.9±2.7	36.6
(28 experiments,	None	Markov	13.9±2.3	29.4
7914 km, mean	Model(35°)	None	9.8±3.0	39.7
epoch 1984.6)	Model	Bias	12.1±2.2	29.6
	Model	Markov	13.6±2.2	29.2
	WVR (20°)	None	12.9±2.9	36.9
	WVR	Bias	13.0±1.8	23.4

	WVR	Markov	13.8±2.3	28.4
GRAS	None	Bias	10.5±2.2	38.8
(73 experiments,	None	Markov	11.2±1.6	27.8
7941 km, mean	Model(35°)	None	12.0±1.9	33.1
epoch 1986.2)	Model	Bias	10.7±2.0	35.4
	Model	Markov	11.2±1.6	27.6
	WVR (20°)	None	12.0±1.7	28.4
	WVR	Bias	11.7±1.5	25.9
	WVR	Markov	12.2±1.5	26.1

[1] The *a priori* information used is either none, or the ground-based model, or the WVR. If an elevation cut-off angle is applied, its value is given in parentheses. If an atmospheric delay is estimated, it is assumed to be either a constant in the zenith direction (bias) or a Markov process.

[2] The standard deviations are scaled so that reduced χ^2 per degree of freedom=1 [*Herring et al.*, 1986].

[3] weighted root-mean-square.

Figure captions

Fig. 1. WVR measurements carried out during four days in November 1986. The large errors in the inferred wet delays from WVR data taken during rain is in this case further increased by water drops forming on the covers of the horn antennas. The error bars for the WVR data have been omitted.

Fig. 2. Simultaneous WVR measurements and Kalman filter estimates of the equivalent zenith wet delay at the Haystack Observatory. The old R-series WVR was used.

Fig. 3. Simultaneous WVR measurements and Kalman filter estimates of the equivalent zenith wet delay at the Mojave VLBI site. The new R-series WVR was used.

Fig. 4. Simultaneous WVR measurements and Kalman filter estimates of the equivalent zenith wet delay at the Onsala Space Observatory. The ASTRID WVR was used.

Fig. 5. Values of a constant atmospheric delay at Onsala estimated in addition to an *a priori* delay consisting of the hydrostatic delay calculated using the total ground pressure and the wet delay inferred from WVR data. The estimation is done for 119 VLBI experiments three times, each time with a different elevation cut-off angle at Onsala in order to check the sensitivity of the estimated value for mapping function errors.

Fig. 6. Weighted RMS residuals of estimated baseline lengths about a "best-fit" straight line. The error bar shows the 90% confidence interval. The hydrostatic delays and the WVR data constitute the *a priori* information used; no estimate of the atmospheric delay at Onsala was made. Seven sets of solutions were made, each with a different elevation cut-off angle at Onsala. The baselines are from Onsala to: Wettzell (Z, 919 km, 72 experiments), Haystack (H, 5600 km, 30 experiments), Westford (W, 5601 km, 96 experiments), Richmond (R, 7307 km, 32 experiments), OVRO (O, 7914 km, 28 experiments), and GRAS (G, 7941 km, 73 experiments).

Fig. 7. Weighted RMS residuals of estimated baseline lengths about a "best-fit" straight line. The hydrostatic delay and the ground based model constitute the *a priori* information used; no estimate of the atmospheric delay at Onsala was made. For the baseline code, see the caption to Figure 6.

Fig. 8. Estimated baseline lengths from Onsala to the "combined" Haystack/Westford site. The circles denote measurements to Haystack and the triangles denote measurements to Westford. Since both sites have been involved in seven experiments simultaneously there are 126 measurements all together. Both the statistical standard error for the individual experiments and the repeatability have improved with time. The following milestones should be noted: June 1982: The Mark-III system at Onsala was upgraded from 7 to 14 videoconverters implying better group-delay measurements; May 1985: Westford installed a cooled receiver and replaced Haystack in almost all CDP experiments; August 1986: Onsala installed a cooled receiver; and March 1987: Onsala installed a dual-frequency feed in the 20m radome enclosed telescope which previously was used for X-band observations only.

Fig. 9. Estimates of the coordinates of Onsala, in a North America fixed frame, in its local North (N), East (E) and Up (U) frame obtained from the analysis of 24 hour VLBI experiments. The squares denote solutions which used stochastic estimation for the atmosphere delays at Onsala; the diamonds denote solutions which used WVR data, excluded data below 20° elevation angle, and did not estimate any atmospheric parameters. The results are given as linear displacements from an arbitrary location. The rates of change of the N and E components predicted by the NUVEL–1 geologic plate–motion model are -9.5 and 17.2 mm/yr, respectively [*DeMets, private communication*, 1987]. The motions of Onsala indicated by these results are probably most sensitive to the velocity of the Wettzell site used in the analysis: The motions of the sites used here were obtained from the preliminary analysis of a much larger VLBI data set [*Herring et al.*, 1989b]; for Wettzell, the horizontal velocities were within 3 mm/yr of the NUVEL–1 velocities and the vertical velocity was -10.2±2.9 mm/yr, consistent with the vertical velocity estimate of -10.6±3.4 mm/yr obtained from the analysis of 5 years of satellite–laser ranging data from the nearby (within 50 m) laser–ranging facility. The WRMS scatter of the heights obtained from the 19 quarter–year laser solutions was 22 mm, about the same as that seen from the VLBI experiments [*Smith et al.*, 1988, and *private communication* 1989].

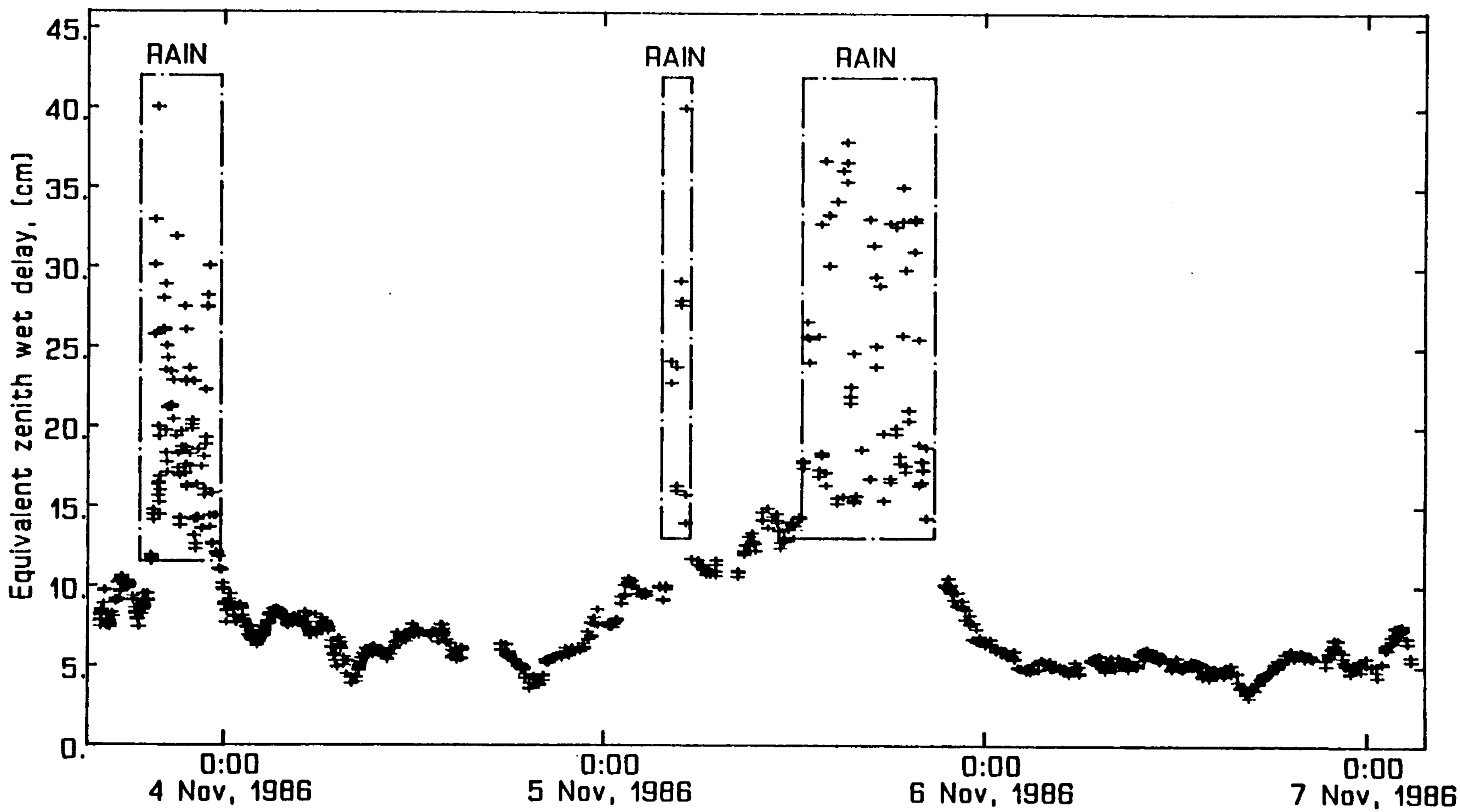
RAIN
RAIN
RAIN
Equivalent zenith wet delay, (cm)
45.
40.
35.
30.
25.
20.
15.
10.
5.
0.
0:00
4 Nov, 1986
0:00
5 Nov, 1986
0:00
6 Nov, 1986
0:00
7 Nov, 1986

Fig 1.

Fig 2.

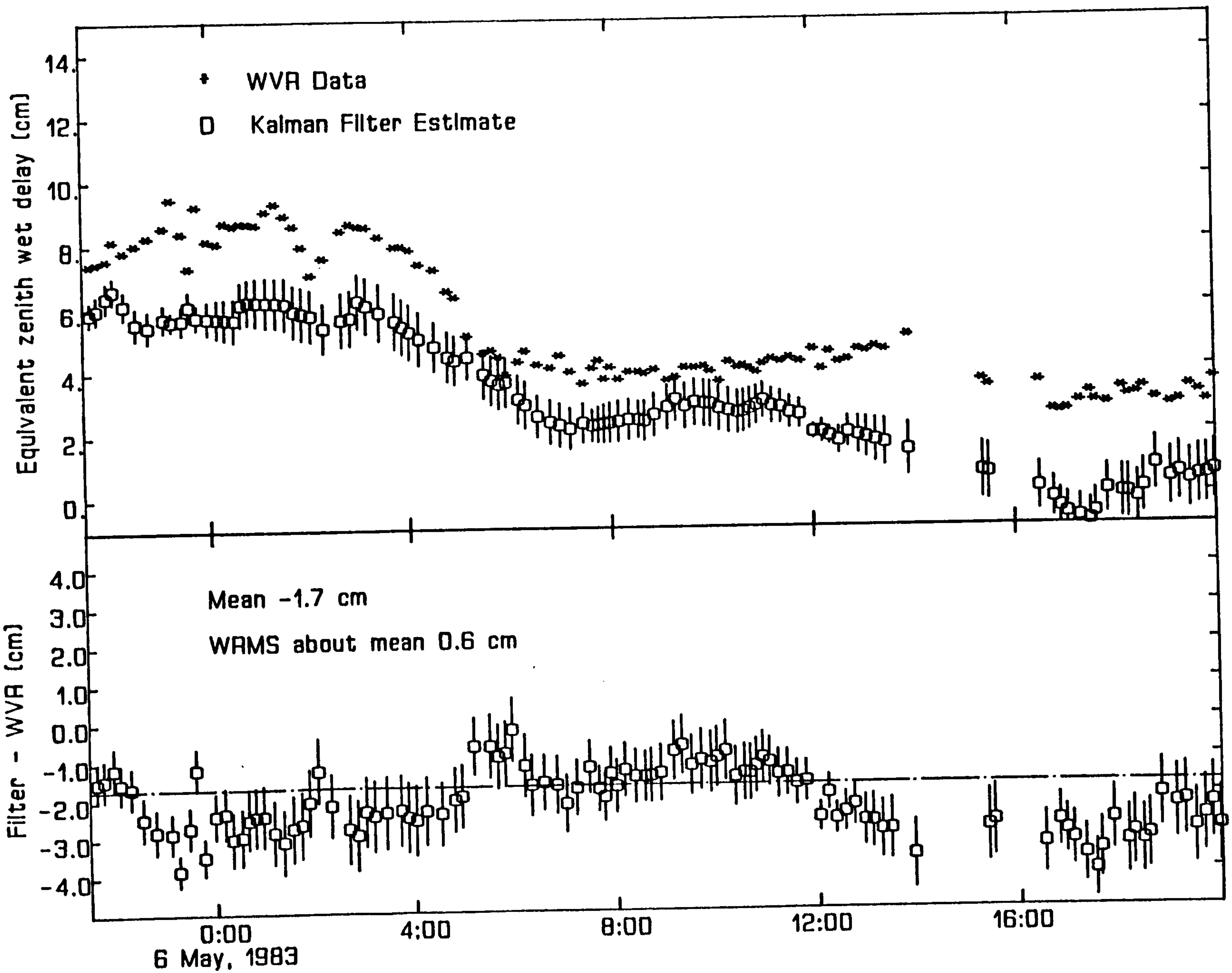

WVR Data
Kalman Filter Estimate
Equivalent zenith wet delay (cm)
14.
12.
10.
8.
6.
4.
2.
0.
Mean -1.7 cm
WRMS about mean 0.6 cm
Filter - WVR (cm)
4.0
3.0
2.0
1.0
0.0
-1.0
-2.0
-3.0
-4.0
0:00
4:00
8:00
12:00
16:00
6 May, 1983

Fig 3

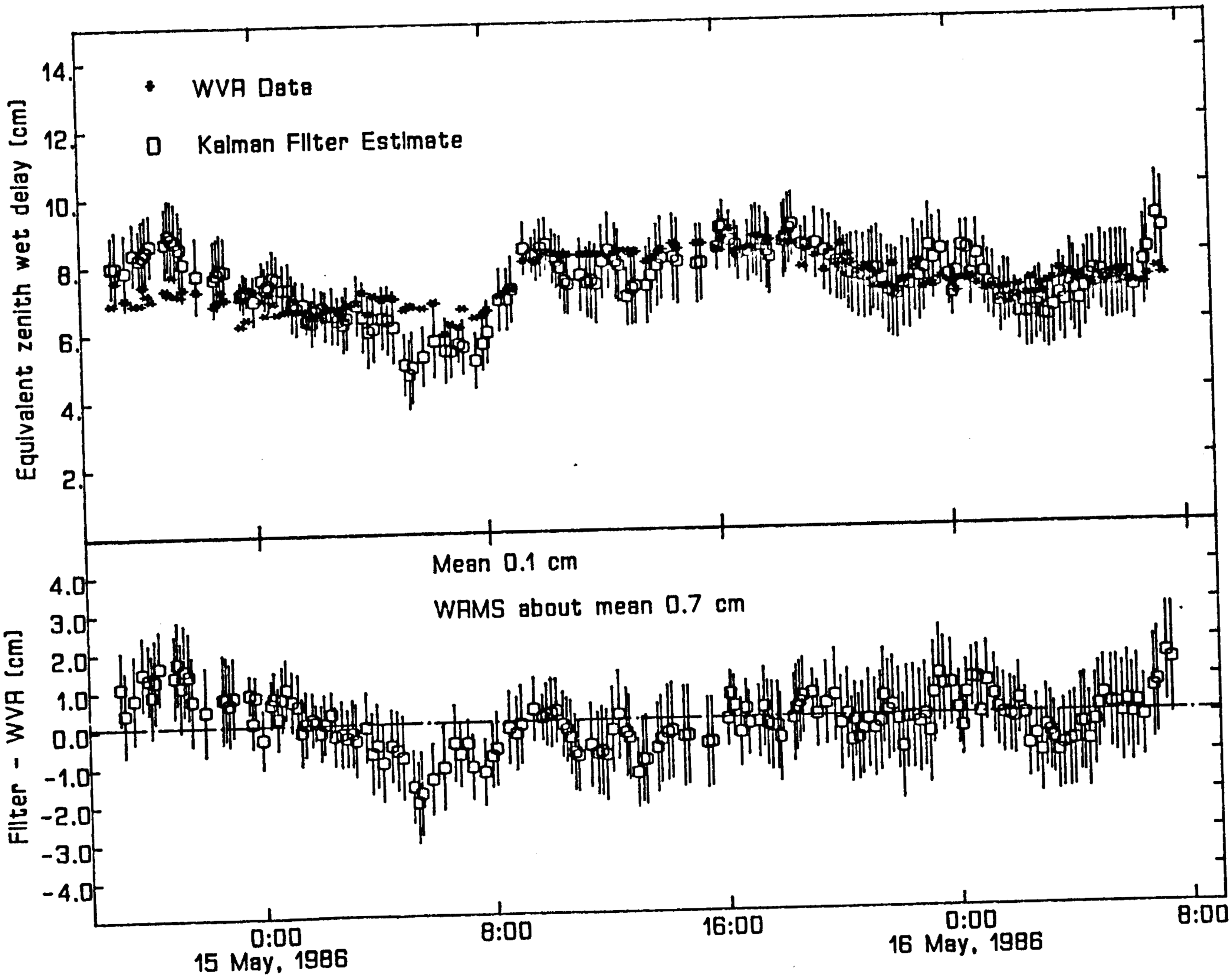

WVR Data
Kalman Filter Estimate
Equivalent zenith wet delay (cm)
14.
12.
10.
8.
6.
4.
2.
Mean 0.1 cm
WRMS about mean 0.7 cm
Filter - WVR (cm)
4.0
3.0
2.0
1.0
0.0
-1.0
-2.0
-3.0
-4.0
0:00
15 May, 1986
8:00
16:00
0:00
16 May, 1986
8:00

Fig 5

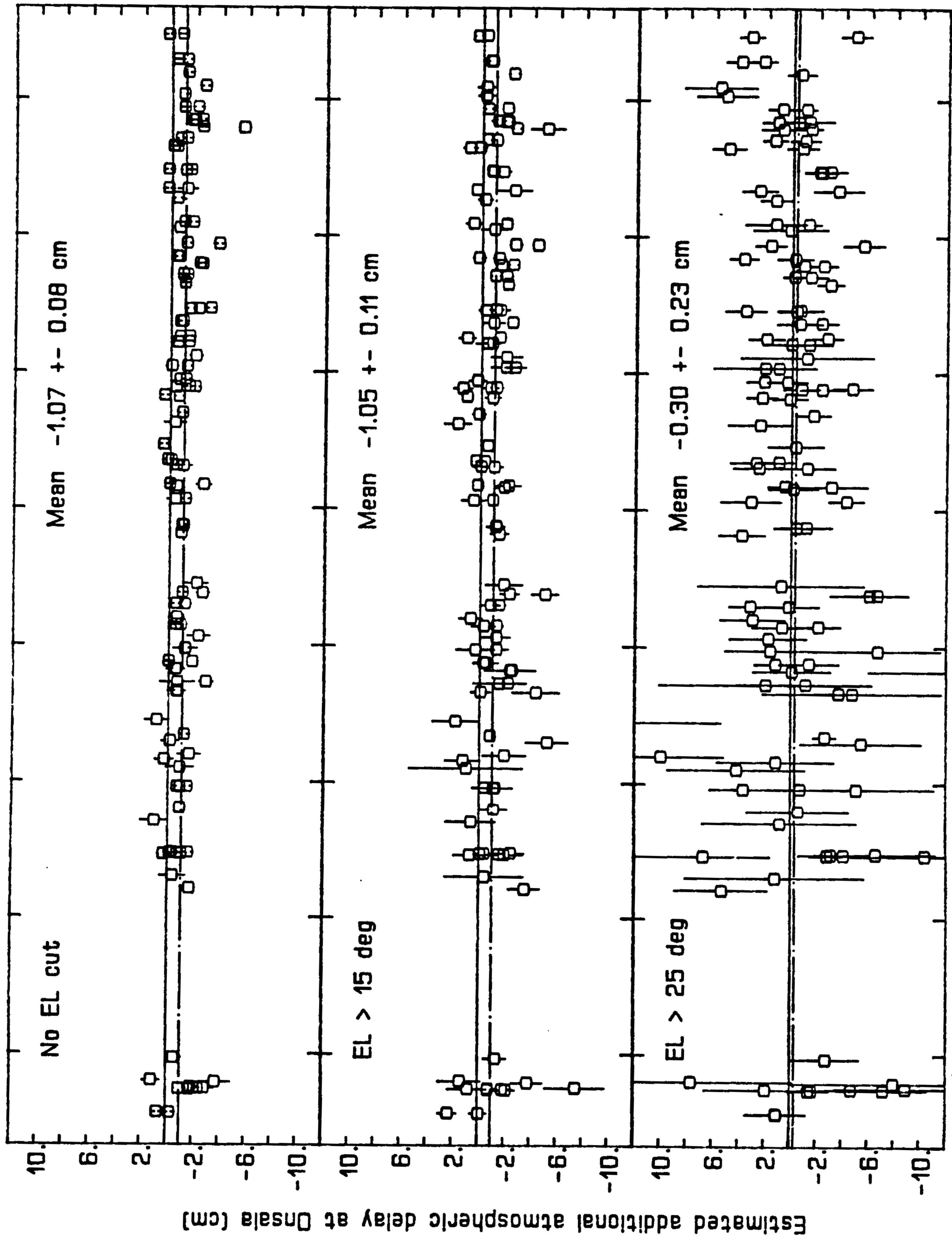

PRECEDING PAGE BLANK NOT FILMED

Fig 6

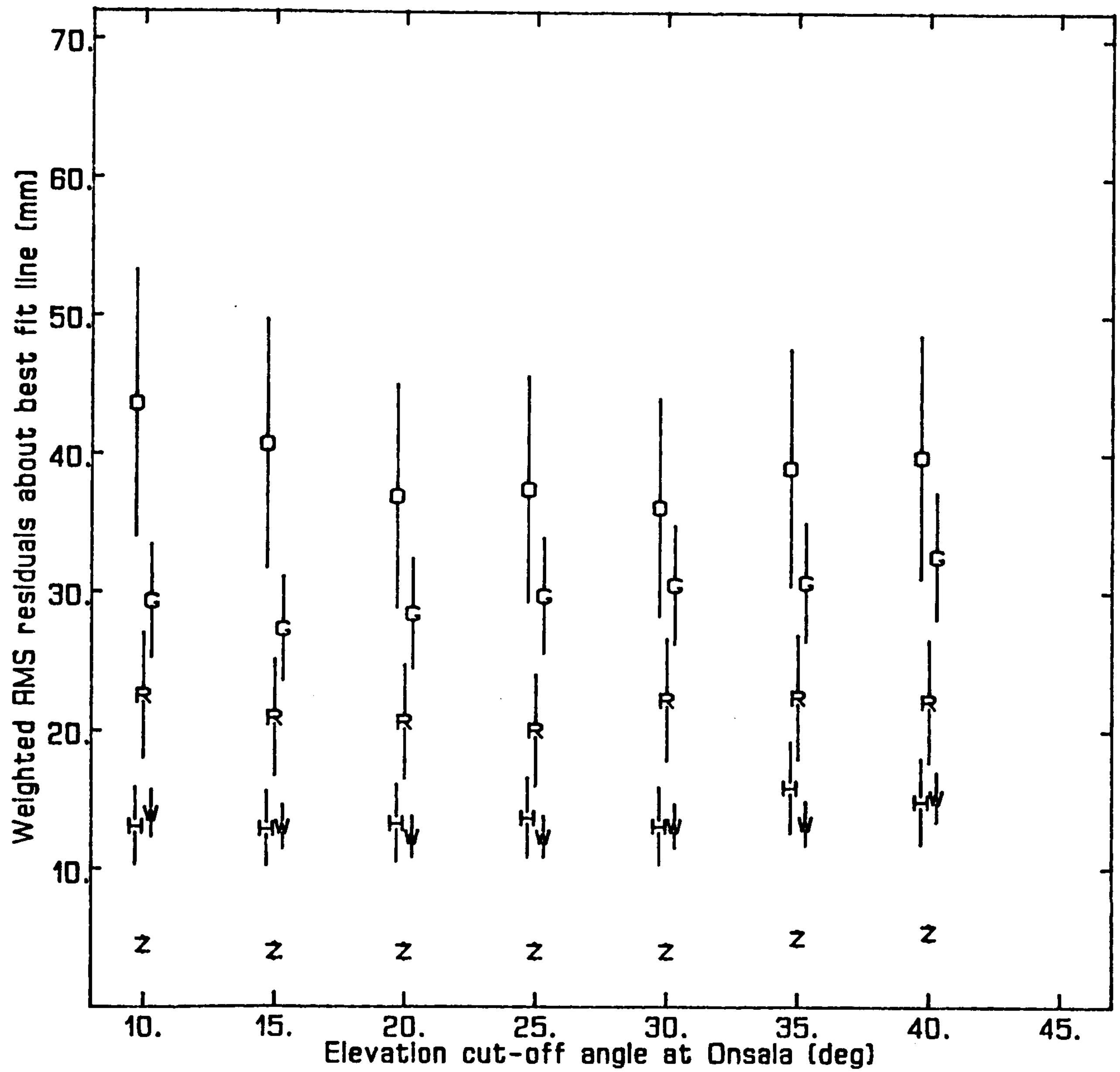
Weighted RMS residuals about best fit line (mm)
70.
60.
50.
40.
30.
20.
10.
10.
15.
20.
25.
30.
35.
40.
45.
Elevation cut-off angle at Onsala (deg)

Fig 7

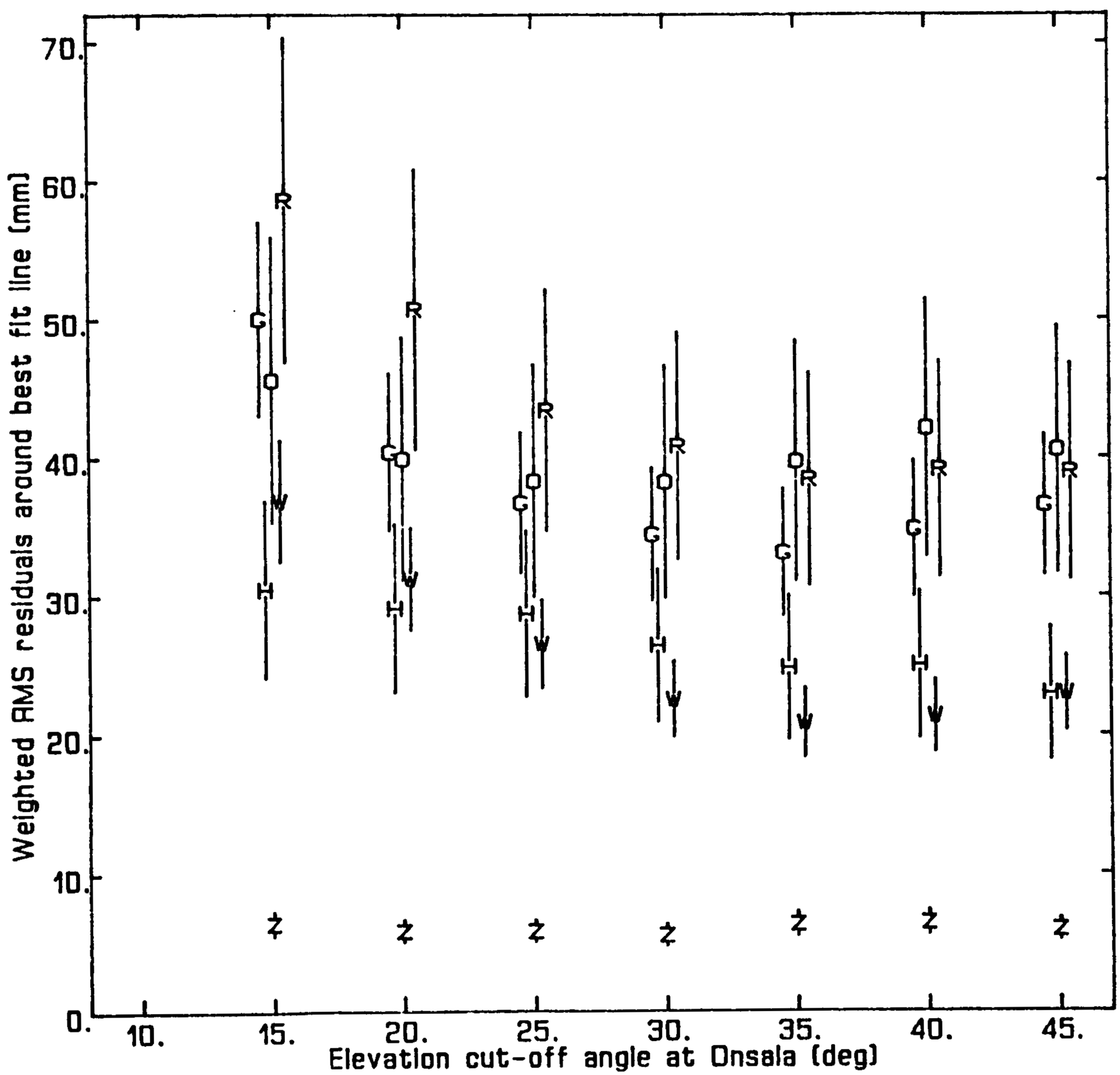

70.
60.
50.
40.
30.
20.
10.
0.
10.
15.
20.
25.
30.
35.
40.
45.
Weighted RMS residuals around best fit line (mm)
Elevation cut-off angle at Onsala (deg)

Fig 8

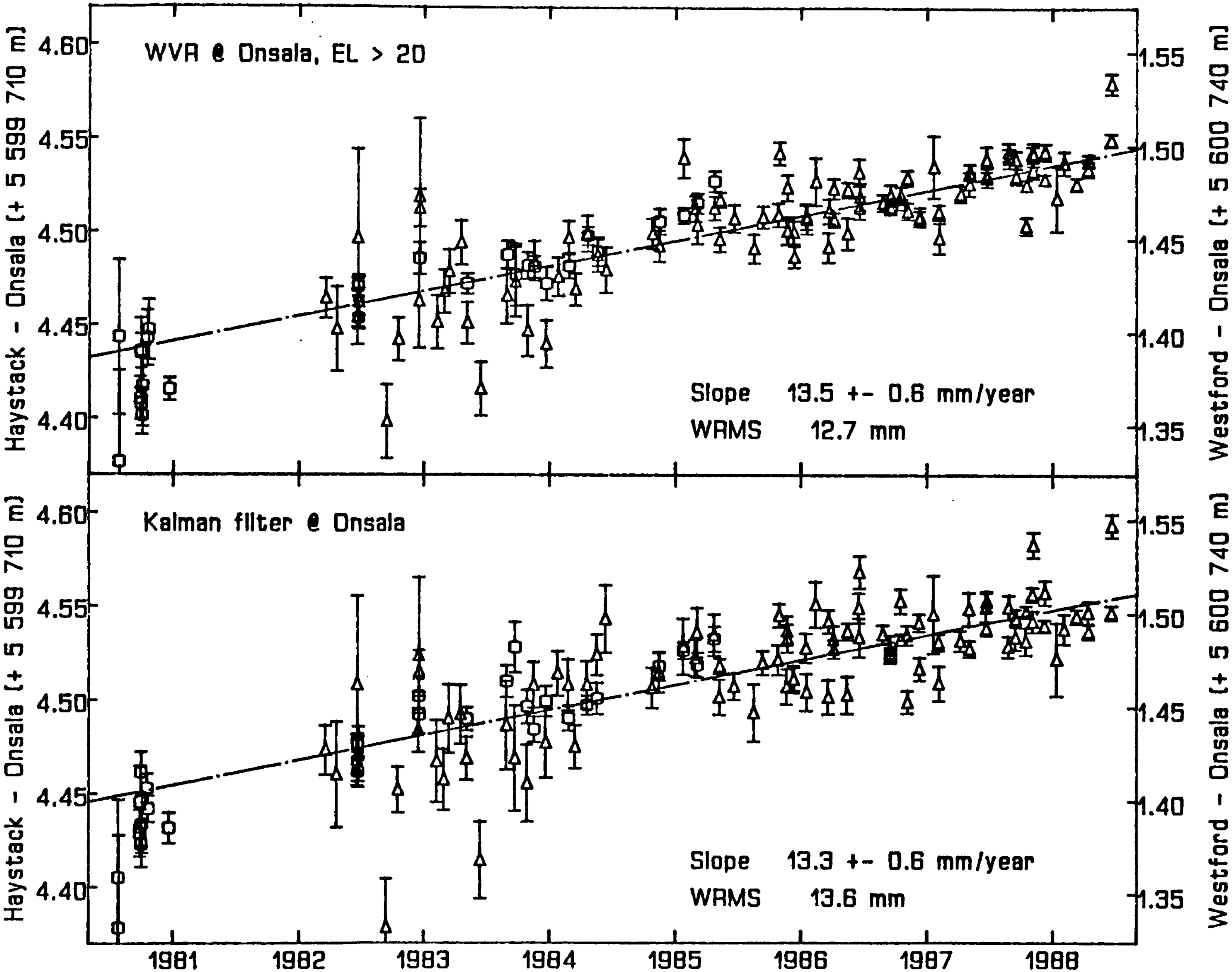
WVR @ Onsala, EL > 20
Slope 13.5 +- 0.6 mm/year
WRMS 12.7 mm
Kalman filter @ Onsala
Slope 13.3 +- 0.6 mm/year
WRMS 13.6 mm
Haystack - Onsala (+ 5 599 710 m)
Westford - Onsala (+ 5 600 740 m)
4.60
4.55
4.50
4.45
4.40
1.55
1.50
1.45
1.40
1.35
1981
1982
1983
1984
1985
1986
1987
1988

Fig 9

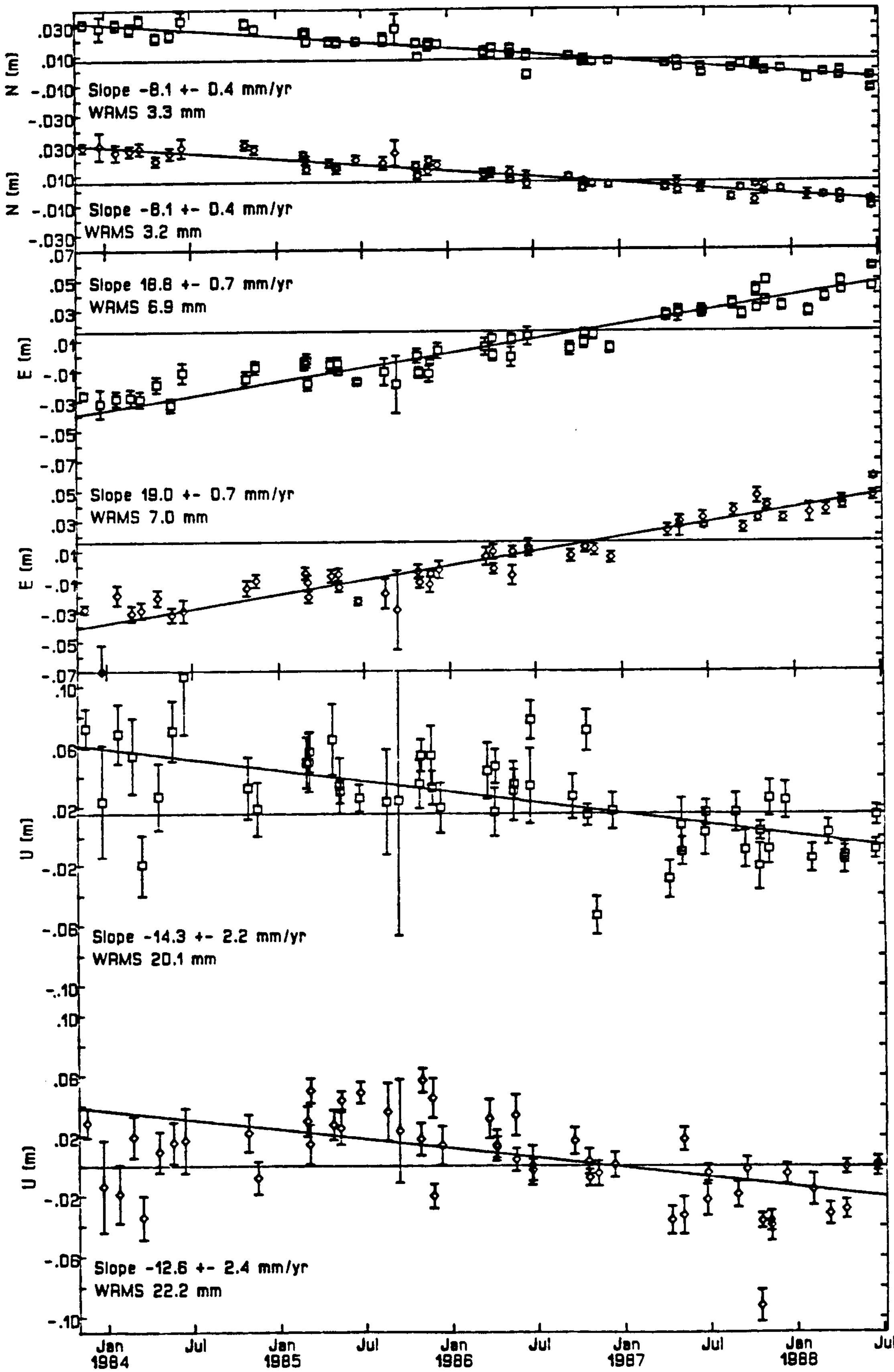

N (m)
.030
.010
-.010
-.030
Slope -8.1 +- 0.4 mm/yr
WRMS 3.3 mm
N (m)
Slope -8.1 +- 0.4 mm/yr
WRMS 3.2 mm
E (m)
.07
.05
.03
.01
-.01
-.03
-.05
-.07
Slope 18.8 +- 0.7 mm/yr
WRMS 6.9 mm
E (m)
Slope 19.0 +- 0.7 mm/yr
WRMS 7.0 mm
U (m)
.10
.06
.02
-.02
-.06
-.10
Slope -14.3 +- 2.2 mm/yr
WRMS 20.1 mm
U (m)
Slope -12.6 +- 2.4 mm/yr
WRMS 22.2 mm
Jan 1984
Jul
Jan 1985
Jul
Jan 1986
Jul
Jan 1987
Jul
Jan 1988
Jul